CIVIL AND ENVIRONMENTAL ENGINEERING REPORTS

E-ISSN 2450-8594

CEER 2024; 34 (4): 0372-0380
DOI: 10.59440/ceer/195335
Original Research Article

ASSESSMENT OF THE LOAD-BEARING CAPACITY OF THE OLD RAILWAY BRIDGE WITH ENCASED STEEL BEAMS

Piotr BILKO[1], Szymon SAWCZYŃSKI
University of Warmia and Mazury in Olsztyn, Faculty of Geoengineering, Olsztyn, Poland

A b s t r a c t

The subject of this study is the inventory and assessment of the load-bearing capacity of a railway bridge. The analysis was conducted on a bridge with a concrete slab reinforced by steel beams as the load-bearing element. The structure is located in the village of Bukowina, Warmian-Masurian Voivodeship, Poland. The aim of the study is to assess the load-bearing capacity of the bridge. The structure's geometry was measured, and its concrete strength class determined. This article presents the results of stress limitation calculations for the tested bridge. Three calculation procedures based on two approaches—a concrete-encased beam and a bending section reinforced with rigid inserts — were applied. The analysis demonstrated that, despite the unesthetic appearance of the bridge, it meets the stress limitation requirements. Though over a hundred years old, the structure remains suitable for use today.

Keywords: load-bearing capacity, technical condition, railway bridge, encased beams

1. INTRODUCTION

In the late 19th and early 20th centuries, rapid development of railway lines took place in what is now the Warmian-Masurian Voivodeship. During this period, numerous short-span bridge structures were built. The primary type of these structures is composite steel-concrete, where steel beams serve as rigid reinforcement for the concrete. Railway bridges with encased filler beams were commonly used for short to medium spans. Structures of this type have been in use in Eastern Europe for over 120 years without significant modifications [1,2,3].

The design methodology of that time considered only the static action of rolled steel beams, while concrete played a reinforcing role. As a result, this load-bearing system still offers a margin of load capacity. Currently, the provisions of PN EN 1994-2 [4] are used to analyse composite bridges. This standard specifies the basic structural, design, and verification requirements based on the limit states concept. The design rules for joist-in-concrete railway bridges are provided in [5].

[1] Corresponding author: University of Warmia and Mazury in Olsztyn, Faculty of Geoengineering, Heweliusz st 4, 10-724 Olsztyn, e-mail: piotr.bilko@uwm.edu.pl

Historical structures of this type were designed and calculated using the permissible stress method. In this paper, archival calculation procedures for cross-sections reinforced with rigid inserts are examined. The first approach was taken from [6]. It is considered appropriate to analyse this type of structure. Older structures were most likely designed according to similar rules. Two selected calculation algorithms for cross-sections with encased steel beams, based on the limit states concept, were also verified. One of them, for example, can be found in [7], which follows the design rules of the UIC code [8]. This standard has been superseded by the current one [5], which is also considered in this paper.

2. BRIDGE CHARACTERISTICS

The subject of the analysis is a railway bridge over a gravel road connecting the villages of Bukowina and Barkweda in the Dywity Commune (Olsztyn County). It is a single-span composite steel-concrete structure (Fig. 1). According to [9], the load-bearing steel beams are supported on rolled steel sections. The formwork is suspended from the beams. The steel beams experience initial deflection under permanent loads before the concrete fully hardens. Once the top layers of the composite are placed, the structure is subjected to traffic loads. Expansion joints separate the deck structure from the bridge abutments, ensuring the free rotation of the bridge deck.

The total span length of the bridge is 6.40 meters, with a support distance of 4.05 meters. The deck is 5.20 meters wide and 0.50 meters thick, and the height to the bottom of the deck is approximately 3.50 meters. A layer of crushed stone, approximately 60 cm thick, was placed on the deck. There are numerous defects in the concrete on the walls and the underside of the slab. However, these defects are not considered alarmingly severe. Small cracks are present on the deck, running parallel to the direction of the steel beams.

Fig. 1. A view of the bridge from the south-east

2.1. Input data for calculations

A Schmidt hammer test was conducted to assess the compressive strength of the concrete. Based on the test results and the relevant standard [10], the characteristic compressive strength of the concrete was estimated to be f_{ck}=26.5 MPa. The width of the flange of the exposed steel beam was measured. It was determined that the cross-sectional reinforcement is an I-beam 'Profile No. 34', which corresponds to the bending characteristics of the current IPN 340 profile [11,12]. The cross-section of the bridge deck is shown in Fig. 2.

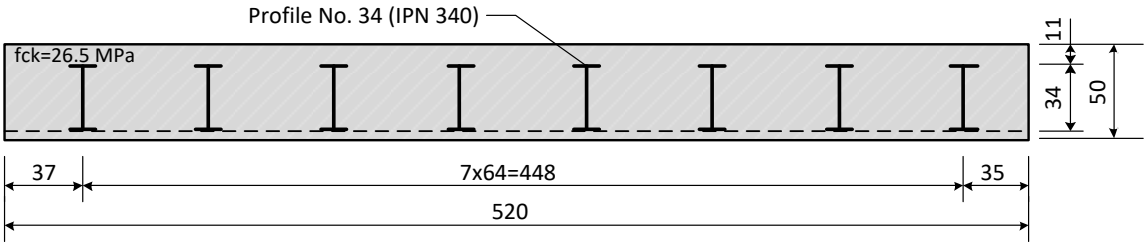

Fig. 2. A Cross-section of the bridge deck

The following parameters were adopted as input data for the calculations (see also Fig.2 and Fig.3):
- theoretical span of the deck: L = 4.25 m,
- deck width: B = 5.20 m,
- section height: d = 0.45 m,
- steel beam spacing: b = 0.64 m,
- thickness of the concrete layer above the upper flange of the steel beam: C_{st} = 0.11 m,
- thickness of the crushed stone layer: t_{st} = 0.60 m,
- track surface: railway sleeper - PS-94, railway rails - UIC 60 (track class: 4 - permissible train speed 60 km/h),
- railway line classification coefficient: α_k = 1.10 according to [13] - for bridges on secondary lines.

The loads are assumed to be uniformly distributed across all beams. The permanent loads are calculated according to [14]. The self-weight (g_1 = 7.60 kN/m) and additional permanent loads (g_2 = 9.50 kN/m) are calculated, respectively. A simply supported beam was adopted as the structural model. The bending moment due to the permanent load acting on a single steel beam before the concrete has fully hardened is M_{g1} = 17.16 kNm. After the concrete has fully hardened, the bending moment on the composite cross-section increases by an additional M_{g2} = 21.45 kNm.
The basic diagram of vertical live loads for bridges is based on the international UIC 71 standard, which can be found, for example, in [13] and [14]. Four forces of 250 kN each are spaced 1.60 m apart and are symmetrically distributed over the section. In this case, only three forces fit on the beam. Based on these assumptions, the bending moment acting on a single steel beam was calculated as M_q = 51.17 kNm.

3. LOAD CAPACITY CALCULATIONS

The stress values in the cross-section were determined using two computational approaches: Procedure A, for a bending cross-section reinforced with rigid inserts, and Procedures B and C, for a highly reinforced, concrete-encased beam. A key issue is the accurate determination of the equivalent characteristics of the composite cross-section. Fig. 3 shows the two static equilibrium models of the

cross-section. Model I assumes full interaction of uncracked concrete in the tension zone, while Model II assumes the concrete in tension is cracked.

The value of $n_{t,i} = E_a/E_{cm,i}$ depends on the load duration and accounts for the influence of the concrete creep phenomenon, where i=0 represents traffic load and i=∞ represents permanent load. Here, E_a is the modulus of longitudinal elasticity of steel, and E_{cm} is the modulus of longitudinal elasticity of concrete. The theoretical assumptions underlying these models are illustrated in Fig. 3.

3.1. Characteristics of the composite section

The composite section is assumed to consist of one beam and a concrete slab with a width equal to the spacing between the beams (b = 0.64 m). The characteristics are calculated for two cases: phase I (Model I), assuming the concrete is uncracked, and phase II (Model II), assuming the concrete in tension is cracked (Fig. 3).

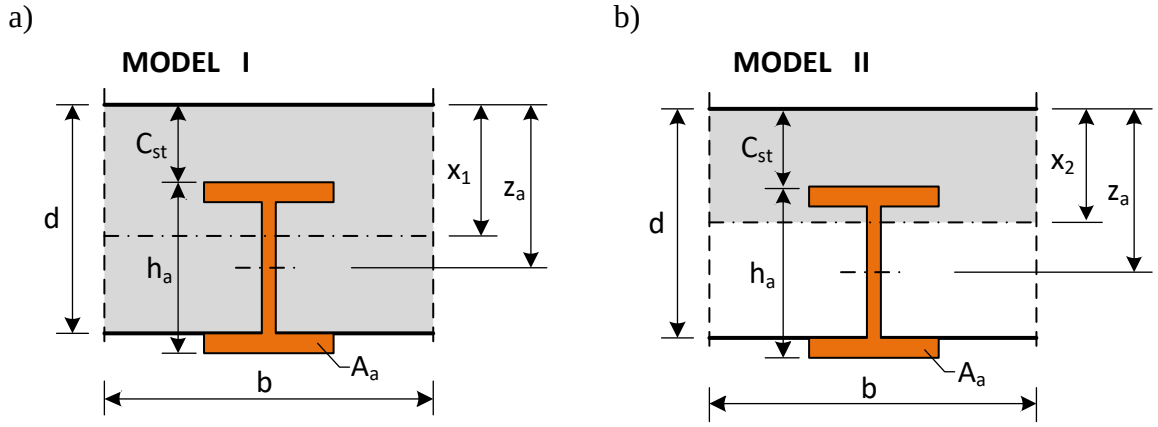

Fig. 3. Definition of the dimensions of the cross-section bridge deck with concrete-encased steel beam: a) interaction of concrete in the tension zone (concrete is uncracked), b) the concrete in tension is cracked

In Model I (Fig. 3a), characteristics of the equivalent cross-section are determined from formulas (3.1) - (3.4):

$$x_I = \frac{n_{t,i} \cdot A_s \cdot z_a + 0.5 \cdot b \cdot d^2}{n_{t,i} \cdot A_s + b \cdot d} \tag{3.1}$$

$$J_I = \frac{b}{3}\left(x_I^3 + (d - x_I)^2\right) + n_{t,i} \cdot J_a + n_{t,i} \cdot A_a \cdot (z_a - x_I)^2 \tag{3.2}$$

$$W_{a,I} = \frac{J_I}{C_{st} + h_a - x_I} \tag{3.3}$$

$$W_{cm,I} = \frac{J_I}{x_I} \tag{3.4}$$

where:

$n_{t,0}$ =6, according to [7], A_a – cross-sectional area of the steel beam, x_I – height of the compression zone, J_I – equivalent moment of inertia of the composite, full interaction of the cross-section, J_a - moment of inertia of the steel beam, $W_{a,I}$ – section modulus of the equivalent cross-section related to the lower fibre of the lower flange, assuming that the concrete is uncracked, $W_{cm,I}$ – section modulus of the equivalent cross-section related to the upper fibre of the concrete, assuming that the concrete is uncracked.

For Model II (Fig. 3b), characteristics of the cross-section are determined as follows:

$$x_{II} = \frac{n_{t,i} \cdot A_s}{b}\left(\sqrt{1+\frac{2 \cdot b \cdot (C_{st} + 0.5 \cdot h_a)}{n_{t,i} \cdot A_s}} - 1\right) \tag{3.5}$$

$$J_{II} = \frac{b}{3} x_{II}^3 + n_{t,i} \cdot J_a + n_{t,i} \cdot A_a \cdot (C_{st} + 0.5 \cdot h_a - x_{II})^2 \tag{3.6}$$

$$W_{a,II} = \frac{J_{II}}{C_{st} + h_a - x_{II}} \tag{3.7}$$

$$W_{cm,II} = \frac{J_{II}}{x_{II}} \tag{3.8}$$

where:
x_{II} – height of the compression zone, J_{II} – equivalent moment of inertia of the of the composite, assuming that the concrete in tension is cracked , $W_{a,II}$ – section modulus of the equivalent cross-section related to the lower fibre of the lower flange, assuming that the concrete in tension is cracked, $W_{cm,II}$ – section modulus of the equivalent cross-section related to the upper fibre of the concrete, assuming that the concrete in tension is cracked.

3.2. Procedure A – concrete reinforced with rigid inserts [6]

According to [6], it is assumed that the concrete in tension is cracked. The geometric characteristics of the equivalent cross-section are determined using formulas (3.5) – (3.8). It is worth noting that when the engineering tables in [6] were created, and even earlier, calculations were performed using the permissible stress method. The stresses could not exceed the material strength (or yield strength) multiplied by a reduction factor. The stress conditions are defined as follows:

$$\sigma_a = \frac{M_{g1}}{W_a} + \frac{n_{t,\infty} \cdot (M_{g2} + M_q)}{W_{a,II}} \le k_a \tag{3.9}$$

$$\sigma_{cm} = \frac{M_{g2} + M_q}{W_{cm,II}} \le k_{cm} \tag{3.10}$$

where:
σ_a – maximum tension stress in steel (the lower fibre of the section), σ_{cm} – maximum compression stress in concrete (the upper fibre of the section), k_a – permissible stresses in steel, k_{cm} – permissible stresses

for concrete. Based on [6], the following values were adopted: k_a = 144.0 MPa and k_{cm} = 9.0 MPa. The ratio of material's elasticity $n_{t,\infty} = E_a/E_{cm}$ is equal to 15 [6].

3.3. Procedure B - concrete-encased beam [7,8]

A heavily reinforced cross-section is analysed, taking into account both cracked and uncracked composite sections. The coefficient γ represents the proportion of tensile concrete in phase I, with the recommended value of γ = 0.5 [8]. The limit states method is used, and the bending moments given in Section 2.1 are multiplied by load coefficients $\gamma_{g(q)}$ according to [14]: γ_{g1} = 1.2, $\gamma_{g2} = \gamma_q$ = 1.5. The stress conditions of steel (at the lower fibre of the cross-section) and concrete (at the upper fibre) are checked against the ultimate limit states (ULS) using the following relationships:

$$\sigma_a = \frac{\gamma_{g1} \cdot M_{g1}}{W_a} + \frac{n_{t,\infty} \cdot \gamma_{g2} \cdot M_{g2} + n_{t,0} \cdot \gamma_q \cdot M_q}{\gamma \cdot W_{a,I} + (1-\gamma) \cdot W_{a,II}} \leq f_{a,d} \tag{3.11}$$

$$\sigma_{cm} = \frac{\alpha_{pl} \cdot (\gamma_{g2} \cdot M_{g2} + \gamma_q \cdot M_q)}{\gamma \cdot W_{cm,I} + (1-\gamma) \cdot W_{cm,II}} \leq f_{cm,d} \tag{3.12}$$

where:
$n_{t,0}$ =6 and $n_{t,\infty}$ =18 according to [7], α_{pl} – concrete plasticity coefficient (assumed 0.75), σ_a – stresses in steel, σ_{cm} – stresses in concrete. The coefficient γ expresses the rate of tensile concrete in phase I. The recommended value is γ = 0.5. The following design strengths were assumed: for steel $f_{a,d}$ = 200 MPa [15], for concrete $f_{cm,d}$ = 17.70 MPa.

3.4. Procedure C – concrete-encased beam [5]

A heavily reinforced cross-section is also considered, with the assumption that the concrete in tension is cracked, unlike in Procedure B (Section 3.3). This procedure also follows the limit states method; however, according to [5], stress limitations are checked for serviceability limit states (SLS). The stress conditions of steel (at the lower fibre of the cross-section) and concrete (at the upper fibre) are checked using the following relationships:

$$\sigma_a = \frac{M_{g1}}{W_a} + \frac{n_{t,\infty} \cdot M_{g2}}{W_{a,II}^{(n_{t,\infty})}} + \frac{n_{t,0} \cdot M_q}{W_{a,II}^{(n_{t,0})}} \leq \frac{f_y}{1.15} \tag{3.13}$$

$$\sigma_{cm} = \frac{M_{g2}}{W_{cm,II}^{(n_{t,\infty})}} + \frac{M_q}{W_{cm,II}^{(n_{t,0})}} \leq 0.6 \cdot f_{ck} \tag{3.14}$$

where:
$W_{a,II}^{(n_{t,0})}, W_{cm,II}^{(n_{t,0})}$ and $W_{a,II}^{(n_{t,\infty})}, W_{cm,II}^{(n_{t,\infty})}$ are calculated for $n_{t,0}$ =6 and $n_{t,\infty}$ =18 respectively, f_y – nominal yield strength (f_y =235MPa), f_{ck} – characteristic compressive strength.

4. RESULTS AND DISCUSSION

This article focuses solely on the stress analysis, determining the stress levels in the composite cross-section. This approach facilitated the comparison of results obtained from selected calculation procedures that have evolved over the years. The authors are aware that for a comprehensive assessment of the bridge's technical condition requires checking all requirements outlined in relevant standards. For instance, EC standards necessitate checking all Ultimate Limit State (ULS) and Serviceability Limit State (SLS) requirements. These requirements, however, were not included in historical regulations.

Three calculation procedures were identified for determining the stresses in cross-sections reinforced with steel beams. The stress values in the boundary fibres of the cross-section were then calculated. The results are summarized in Table 1, which presents the calculated stress values. Additionally, due to the different calculation methods, the values of the section moduli for the equivalent cross-section are also included.

Table 1. The results of the stress calculations

	Section moduli of the equivalent cross-section				Stress values (effort)	
	$W_{a,I}$ [cm^3]	$W_{cm,I}$ [cm^3]	$W_{a,II}$ [cm^3]	$W_{cm,II}$ [cm^3]	Steel σ_a [MPa]	Concrete σ_{cm} [MPa]
Procedure A $n_{t,\infty}=15$	-	-	18780.5	25558.4	76.58 (53%)	2.84 (32%)
Procedure B $n_{t,0}=6$	27403.9	25428.1	8383.0	17274.8	80.40 (40%)	3.83 (22%)
Procedure C $n_{t,0}=6$ $n_{t,\infty}=18$	27403.9 38859.0	25428.1 32710.7	8383.0 22026.5	17274.8 27810.0	65.14 (32%)	3.62 (23%)

Tab. 1 presents the values of permissible stresses on the tensioned lower edge of the steel beams and the compressive upper edge of the concrete slab for Procedures I and II. The values in brackets represent the degree of material effort calculated using equations (3.9) – (3.10), (3.11) – (3.12), and (3.13) – (3.14) for Procedures A, B, and C, respectively. The lowest degree of stress in the cross-section (steel – 32%, concrete – 23%) was obtained for historical design requirements – Procedure C, whereas the highest degree of stress (steel – 53%, concrete – 32%) was obtained for currently applicable regulations – Procedure A. Similar values to those of Procedure C were obtained using Procedure B (steel – 40%, concrete – 22%), meaning the requirements of outdated design standards. The calculations indicate a rather low level of stress in the bridge cross-section.

The analysis of the bridge's load-bearing capacity confirms its adequacy for use. To increase the width of the road under the bridge, the infrastructure manager decided to rebuild the structure. A new bridge was built to replace the analysed one. The view of the new bridge is shown in Fig. 4.

Fig. 4. A view of the bridge from the south-east after renovation

5. SUMMARY AND CONCLUSIONS

Various calculation methods are available for analysing the load-bearing capacity of a railway bridge. This work presents two calculation procedures. These procedures demonstrated the load-bearing capacity reserve of the analysed structure. The procedure in [6] was likely used when the bridge was designed, as it provides the correct mathematical description for steel beam-reinforced structures. Access to obsolete, historical calculation procedures is limited, and properly identifying the type of cross-section reinforcement also presents challenges. As a result, these structures are difficult to analyse.

Newly designed structures can be calculated using various procedures and algorithms, reflecting the evolution of computational methodologies over time. However, there is no thorough, comprehensive study organizing the issues related to this type of construction. This article demonstrates the assessment of the load-bearing capacity of an old railway bridge with encased steel beams using different computational approaches.

REFERENCES

1. Kvočák, V et al. 2013. State of the Art in the Utilization of Deck Bridges with Encased Filler-Beams in the Standard Construction Practice. *Journal Of Civil Engineering*, **Vol. 8, Issue 1**, 2013, pp. 107-114.
2. Odrobiňák, J et al. 2012. Study on Short Span Deck Bridges with Encased Steel Beams, *Procedia Engineering*, **Volume 40**, 2012,pp. 333-338, https://doi.org/10.1016/j.proeng.2012.07.104.
3. Vičan, J et al. 2012. Analysis and Load-carrying Capacity Estimation of Existing Railway Filler-beam Deck Bridges, *Journal Of Civil Engineering*, **Vol. 7, Issue 2**, 2012, pp. 5-14.
4. PN-EN 1994-2: Eurocode 4: Design of Composite Steel and Concrete Structures. Part 2: General Rules and Rules for Bridges.

5. UIC Code 773 Ed. 5 – Recommendations for the Design of Joist-In-Concrete Railway Bridges. International Union of Railways (UIC), 2010.
6. Bryl, S 1954. Tablice inżynierskie. Tom II. Konstrukcje mostowe – fundamenty [Engineering Tables. Volume II. Bridge Structures – Foundations]. *Państwowe Wydawnictwo Naukowe*. Poznań.
7. Karlikowski, J et al. 2003. *Mostowe konstrukcje zespolone stalowo-betonowe zasady projektowania [Bridge composite steel-concrete structures, design principles]*. Warszawa: Wydawnictwa Komunikacji i Łączności.
8. UNION INTERNATIONALE DES CHEMINS DE FER. Recommendations for the Design of Joist-In Concrete Railway Bridges. UIC, Paris, 1982, 773 R 3rd edition.
9. Kersten, C 1912. *Brücken in Eisenbeton, Teil 1: Platten- und Balkenbrücken [Reinforced Concrete Bridges, Part 1: Slab and Beam Bridges]*. Verlag Von Wilhelm Ernst &Sohn, Berlin.
10. PN-EN 13791:2008 Ocena wytrzymałości betonu na ściskanie w konstrukcjach i prefabrykowanych wyrobach betonowych [Assessment of concrete compressive strength in structures and prefabricated concrete products].
11. Final Report Part I of the Research Programme "Steel in Old Buildings and Residential Construction" *[Abschlussbericht Teil I zum Forschungsprogramm „Stahl im Altbau und Wohnungsbau"]*, Versuchsanstalt Für Stahl, Holz Und Steine, Karlsruhe, 1979.
12. Czapliński, K 2009. *Dawne wyroby ze stopów żelaza [Old cast iron and steel constructions],* Dolnośląskie Wydawnictwo Edukacyjne, Wrocław.
13. PN-EN 1991-2:2007 Eurocode 1: Actions on structures - Part 2: Traffic loads on bridges.
14. PN-85/S-10030 Obiekty mostowe – Obciążenia [Bridge structures – Loads], 1985.
15. PN-S-10052:1982 Obiekty mostowe - Konstrukcje stalowe – Projektowanie [Bridge structures - Design of Steel Structures], 1982.